AN INTERFACE CRACK WITH MIXED ELECTRO-MAGNETIC CONDITIONS
AT IT FACES IN A PIEZOELECTRIC / PIEZOMAGNETIC BIMATERIAL
UNDER ANTI-PLANE MECHANICAL AND IN-PLANE ELECTRIC LOADINGS

Oleg ONOPRIIENKO[*], Volodymyr LOBODA[*], Alla SHEVELEVA[**], Yuri LAPUSTA[***]

[*]Department of Theoretical and Applied Mechanics, Oles Honchar Dnipro National University, Gagarin Av., 72, Dnipro 49010, Ukraine
[**]Department of Computational Mathematics, Oles Honchar Dnipro National University, Gagarin Av., 72, Dnipro 49010, Ukraine
[***]Université Clermont Auvergne, SIGMA Clermont (ex- IFMA, French Institute of Advanced Mechanics),
Institut Pascal, BP 10448, F-63000 Clermont-Ferrand, France, CNRS, UMR 6602, IP, F-63178 Aubière, France

onopriienko.oleg@gmail.com, loboda@dnu.dp.ua, allasheveleva@i.ua, lapusta@sigma-clermont.fr

Abstract: An interface crack between two semi-infinite piezoelectric/piezomagnetic spaces under out-of-plane mechanical load and in-plane electrical and magnetic fields parallel to the crack faces is considered. Some part of the crack faces is assumed to be electrically conductive and having uniform distribution of magnetic potential whilst the remaining part of the crack faces is electrically and magnetically permeable. The mechanical, electrical, and magnetic factors are presented via functions which are analytic in the whole plane except the crack region. Due to these representations the combined Dirichlet-Riemann and Hilbert boundary value problems are formulated and solved in rather simple analytical form for any relation between conductive and permeable zone lengths. Resulting from this solution the analytical expressions for stress, electric and magnetic fields as well as for the crack faces displacement jump are presented. The singularities of the obtained solution at the crack tips and at the separation point of the mention zones are investigated and the formulas for the corresponding intensity factors are presented. The influence of external electric and magnetic fields upon the mechanic, electric and magnetic quantities at the crack region are illustrated in graph and table forms.

Keywords: Piezoelectromagnetic Material, Mode-III Interface Crack, Analytical Solution

1. INTRODUCTION

Piezoelectromagnetic materials are often used as functional parts of different engineering systems including sensors, transducers and actuators. However, existing micro-defects and particularly interface cracks can strongly reduce their strength. For this reason, interface cracks in piezoelectric and piezoelectomagnetic materials have been actively studying in the last several decades. A certain attention in this period was devoted to plane interface crack problem. Particularly, concerning piezoelectomagnetic materials this problem was developed in paper by Fan et al., (2009) and Feng et al., (2010). Different variants of electrical and magnetic conditions at the crack faces of an interface crack with a contact zone in a magnetoelectroelastic bimaterial under mechanical, electric and magnetic loads were considered by Herrmann et al., (2010), Feng et al., (2011, 2012), and Ma et al., (2012). Additional accounting of thermal flux for an interface crack in a magnetoelectroelastic bimaterial were performed in papers of Ma et al., (2011) and Feng et al., (2012). Modelling of the pre-fracture zone for an interface crack between two dissimilar magnetoelectroelastic materials was done by Ma et al., (2013). The electrically impermeable and magnetically permeable conditions at the crack faces were considered in this paper.

It is known (Parton and Kudryavtsev, 1988) that an in-plane electric or magnetic field induces the out-of-plane deformation for piezoelectric and piezoelectomagnetic material with certain directions of polarization. On this reason an investigation of such kind of deformation, particularly the mode III cracks, is more important for the mentioned materials than for electrically and magnetically passive ones. The mode III interface crack problem for dissimilar piezo-electromagneto-elastic bimaterial media with taking into account the electro-magnetic field inside the crack was investigated by Li and Kardomateas (2006) for impermeable and permeable crack models. A closed-form solution for anti-plane mechanical and in-plane electric and magnetic fields for a crack between two dissimilar magnetoelectroelastic materials was obtained in papers by Wang and Mai (2006, 2008) for the two extreme cases of an impermeable and a permeable crack. The anti-plane deformation of the multilayered piezomagnetic/piezoelectric composite with periodic interface cracks, subjected to in-plane magnetic or electric fields, was studied by Wan et al., (2012a) and Wan et al., (2012b) analyzed the mode III crack crossing the magnetoelectroelastic bimaterial interface under concentrated magnetoelectromechanical loads. The behaviour of two collinear and also parallel symmetry and non-symmetric interface cracks in magneto–electro–elastic materials under an anti-plane shear stress loading was by studied by Zhou et al., (2004, 2007a, 2009) with use of Schmidt method. The solutions of a limited-permeable crack or two collinear limited-permeable cracks in piezoelectric/ piezomagnetic materials subjected to a uniform tension loading were investigated in paper by Zhou et al., (2007b) using the generalized Almansi's theorem. Anti-plane problem for an impermeable or permeable interface crack between two dissimilar magnetoelectroelastic plates subjected to anti-plane mechanical and in-plane magneto-electrical loads was investigated by Su and

sciendo

Oleg Onopriienko, Volodymyr Loboda, Alla Sheveleva, Yuri Lapusta   DOI 10.2478/ama-2018-0046
An Interface Crack with Mixed Electro-Magnetic Conditions at it Faces in a Piezoelectric/ Piezomagnetic Bimaterial under Anti-Plane Mechanical and In-Plane Electric Loadings

Feng (2008). Multiferroic interface fracture of piezomagnetic/ piezoelectric composite under magnetic and electric loadings was considered by Li and Lee (2010). Shi et al., (2013) investigated arc-shaped interface cracks between a functionally graded magneto-electro-elastic layer and an orthotropic elastic substrate under anti-plane shear load. Single and periodic mode-III cracks moving along the interface of piezoelectric-piezomagnetic bimaterial were considered by Chen et al., (2012) and Yue and Wan (2014), respectively. Also the case of a moving interface crack between magnetoelectroelastic and functionally graded elastic layers was studied by Hu and Chen (2014). An exact analytic solution to the anti-plane problem for a non-homogeneous bimaterial medium containing closed interfacial cracks, which faces can move relatively to each other with dry friction under the action of arbitrary single loading and also cyclic loading was considered by Sulym et al., (2015a, 2015b). A more detailed review of anti-plane crack problem investigation in piezoelectric/piezomagnetic bimaterials is presented in Govorukha et al., (2016).

Temporary actuators and other electronic devices are often constructed with use of thin film electrodes sandwiched between piezoelectric layers. Such electrodes are usually prepared of a metal powder, conducting polymers etc. and do not change the mechanical properties of matrixes (Ru, 2000). Delamination of the mentioned electrodes leads to the appearance of conducting interface cracks. For a plane case a conductive interface crack in a piezoelectric bimaterial was considered by Beom and Atluri (2002) and Loboda et al., (2014) for "open" and contact zone crack models, respectively. For an out-of-plane conductive interface crack the results of the papers Wang and Zhong (2002) and Wang et al., (2003) specifying the oscillating singularity at the crack tips are valid. However in many cases only some part of the crack faces can be conductive because of interface electrode delamination while on remaining part some other kind of electrical conditions can take place. Accounting of such mixed electrical conditions at the crack faces leads to more complicated problem than for uniform ones. The crack with mixed (conductive-permeable) conditions at the crack faces was considered for a piezoelectric bimaterial by Lapusta et al., (2017). However, for a piezoelectric/ piezomagnetic bimaterials this important situation has not been studied before and it comprises the main subject of the present paper. In spite of this case is more complicated than the piezoelectric one, an exact solution of the problem was found.

2. BASIC FORMULAS FOR PEMM (PIEZO-ELECTRO-MAGNETIC MATERIAL) FOR ANTI-PLANE CASE

The constitutive relations for the piezo-electro-magnetic material are (Sih and Song, 2003):

$$\sigma_{ij} = c_{ijks}\varepsilon_{ks} - e_{sij}E_s - h_{sij}H_s,$$

$$D_i = e_{iks}\varepsilon_{ks} + \alpha_{is}E_s + d_{is}H_s,$$

$$B_i = h_{iks}\varepsilon_{ks} + d_{is}E_s + \gamma_{is}H_s,$$

where σ_{ij}, ε_{ij} – components of stress and strain tensors, D_i, B_i – components of the electric and magnetic inductions, E_i, H_i – intensities of the electric and magnetic fields, c_{ijks} – elastic, e_{iks} – piezoelectric, h_{iks} – piezomagnetic, d_{is} – electromagnetic constants, α_{is}, γ_{is} – electric and magnetic permeabilities.

The equilibrium equations in the absence of body forces and free charges are:

$$\sigma_{ij,j} = 0, D_{i,i} = 0, B_{i,i} = 0.$$

The expressions for the deformation, electric and magnetic fields have the form:

$$\varepsilon_{ij} = \tfrac{1}{2}(u_{i,j} + u_{j,i}), E_i = -\phi_{,i}, H_i = -\psi_{,i},$$

where u_i – the components of the displacement vector, ϕ, ψ – the electric and magnetic potentials, comma means differentiation on the respective coordinate.

In an anti-plane case we have:

$$u_1 = u_2 = 0, u_3 = u_3(x_1, x_2),$$

$$\phi = \phi(x_1, x_2), \psi = \psi(x_1, x_2).$$

Then, the constitutive relations take the form:

$$\begin{pmatrix} \sigma_{3i} \\ D_i \\ B_i \end{pmatrix} = \mathbf{R} \begin{pmatrix} u_{3,i} \\ -\phi_{,i} \\ -\psi_{,i} \end{pmatrix}, \mathbf{R} = \begin{pmatrix} c_{44} & e_{15} & h_{15} \\ e_{15} & -\alpha_{11} & -d_{11} \\ h_{15} & -d_{11} & -\gamma_{11} \end{pmatrix},$$

where $i = 1,2$.

Introducing the vectors:

$$\mathbf{u} = [u_3, \phi, \psi]^T, \mathbf{t} = [\sigma_{32}, D_2, B_2]^T, \tag{1}$$

one can write

$$\mathbf{t} = \mathbf{R}\mathbf{u}_{,2}. \tag{2}$$

As the functions u_3, ϕ and ψ are harmonic, then taking into account (2), the following presentations are valid:

$$\mathbf{u} = \Phi(z) + \overline{\Phi}(\bar{z}),$$

$$\mathbf{t} = \mathbf{B}\Phi'(z) + \overline{\mathbf{B}}\overline{\Phi}'(\bar{z}), \tag{3}$$

where: $\Phi(z) = [\Phi_1(z), \Phi_2(z), \Phi_3(z)]^T$ – an arbitrary analytical vector-function of the complex variable $z = x_1 + ix_2$, $\mathbf{B} = i\mathbf{R}$.

3. FORMULATION OF THE PROBLEM AND BASIC FORMULAS FOR A BIMATERIAL COMPOUND

Assume that the crack is located in the interval $[c, b]$ of the material separation line (Fig. 1). Suppose also that the section $[c, a]$ of the crack faces is covered with electrodes, which, moreover, maintain a constant distribution of the magnetic field. It means that the conditions on this section can be written in the form:

$$\sigma_{32}^{(1)} = \sigma_{32}^{(2)} = 0, E_1^{(1)} = E_1^{(2)} = 0,$$

$$H_1^{(1)} = H_1^{(2)} = 0 \text{ for } c < x_1 < a. \tag{4}$$

The remaining part of the crack is assumed to be free from electrodes. Therefore, because of the absence of the crack opening in x_2 direction this part of crack faces should be considered as electrically and magneto permeable. Thus, one gets the following conditions:

$$\sigma_{32}^{(1)} = \sigma_{32}^{(2)} = 0, \langle D_2 \rangle = 0, \langle B_2 \rangle = 0,$$

$$\langle E_1 \rangle = 0, \langle H_1 \rangle = 0 \text{ for } a < x_1 < b, \tag{5}$$

where $\langle \bullet \rangle$ means the jump of the function via material interface.
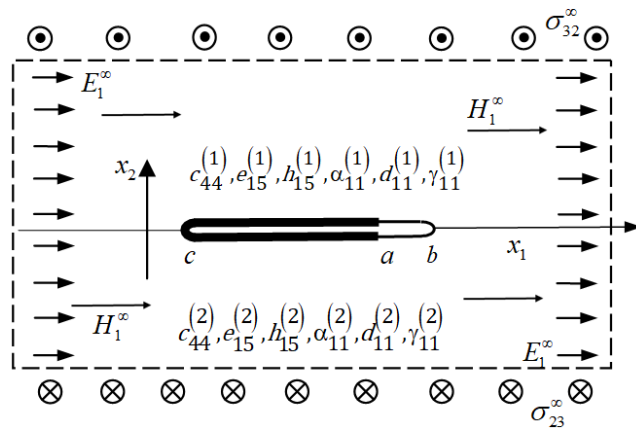
Fig. 1. A crack between two piezoelectromagnetic materials

The crack described above may arise due to a soft multi-layered electrode exfoliation, made of ferro-magnetic material, situated at the interval $[c, a]$, with the additional exfoliation of the interval $[a, b]$ of the non-electroded interface. Electric and magnetic conditions used in (4), (5) can be considered as a certain approximation of real conditions taking place at the interface crack faces in piezoelectromagnetic bimaterials. However in many cases these conditions model electric and magnetic state at these faces with sufficient accuracy Wang and Mai (2008). It's also assumed, that the vector $P^\infty = [\sigma_{32}^\infty, E_1^\infty, H_1^\infty]^T$ is given at infinity.

Introducing the vectors:

$$\mathbf{v}' = [u_3', D_2, B_2]^T, \ \mathbf{P} = [\sigma_{32}, \phi', \psi']^T \tag{6}$$

(the derivatives in (6) are implicit on x_1), on the basis of (3) we have:

$$\mathbf{v}' = \mathbf{M}\Phi'(z) + \bar{\mathbf{M}}\bar{\Phi}'(\bar{z}), \tag{7}$$

$$\mathbf{P} = \mathbf{N}\Phi'(z) + \bar{\mathbf{N}}\bar{\Phi}'(\bar{z}), \tag{8}$$

where the matrixes $\mathbf{M}$ and $\mathbf{N}$ have the structure:

$$\mathbf{M} = \begin{pmatrix} 1 & 0 & 0 \\ B_{21} & B_{22} & B_{23} \\ B_{31} & B_{32} & B_{33} \end{pmatrix}, \mathbf{N} = \begin{pmatrix} B_{11} & B_{12} & B_{13} \\ 0 & 1 & 0 \\ 0 & 0 & 1 \end{pmatrix}.$$

For a bimaterial compound the relations (7), (8) can be written in the form:

$$\mathbf{v}'^{(k)} = \mathbf{M}^{(k)}\Phi'^{(k)}(z) + \bar{\mathbf{M}}^{(k)}\bar{\Phi}'^{(k)}(\bar{z}), \tag{9}$$

$$\mathbf{P}^{(k)} = \mathbf{N}^{(k)}\Phi'^{(k)}(z) + \bar{\mathbf{N}}^{(k)}\bar{\Phi}'^{(k)}(\bar{z}), \tag{10}$$

where $k = 1$ for the area 1 and $k = 2$ for the area 2; $\mathbf{M}^{(k)}$ and $\mathbf{N}^{(k)}$ are the matrixes $\mathbf{M}$ and $\mathbf{N}$ for the areas 1 and 2, respectively; $\Phi^{(k)}(z)$ are arbitrary vector-functions, analytic in the areas 1 and 2, respectively.

Next we require that the equality $P^{(1)} = P^{(2)}$ holds true on the entire axis x_1. Then it follows from (10):

$$\mathbf{N}^{(1)}\Phi'^{(1)}(x_1 + i0) + \bar{\mathbf{N}}^{(1)}\bar{\Phi}'^{(1)}(x_1 - i0) =$$

$$= \mathbf{N}^{(2)}\Phi'^{(2)}(x_1 - i0) + \bar{\mathbf{N}}^{(2)}\bar{\Phi}'^{(2)}(x_1 + i0). \tag{11}$$

Here we have used the designation $F(x_1 \pm i0) = F^\pm(x_1)$, which means the limit value of a function $F(z)$ at $x_2 \to 0$ from above or below, respectively.

The equation (11) can be written as:

$$\mathbf{B}^{(1)}\Phi'^{(1)}(x_1 + i0) - \bar{\mathbf{B}}^{(2)}\bar{\Phi}'^{(2)}(x_1 + i0) =$$

$$= \mathbf{B}^{(2)}\Phi'^{(2)}(x_1 - i0) - \bar{\mathbf{B}}^{(1)}\bar{\Phi}'^{(1)}(x_1 - i0).$$

The left and right sides of the last equation can be considered as the boundary values of the functions:

$$\mathbf{N}^{(1)}\Phi'^{(1)}(z) - \bar{\mathbf{N}}^{(2)}\bar{\Phi}'^{(2)}(z)$$

and:

$$\mathbf{N}^{(2)}\Phi'^{(2)}(z) - \bar{\mathbf{N}}^{(1)}\bar{\Phi}'^{(1)}(z), \tag{12}$$

which are analytic in the upper and lower planes, respectively. But it means that there is a function $\Pi(z)$, which is equal to the mentioned functions in each half-plane and is analytic in the entire plane.

Assuming $\Pi(z)|_{z\to\infty} \to 0$, on the basis of the Liouville theorem we find that each of the functions (12) is equal to 0 for each z from the corresponding half-plane. Hence, we obtain:

$$\bar{\Phi}'^{(2)}(z) = \left(\bar{\mathbf{N}}^{(2)}\right)^{-1}\mathbf{N}^{(1)}\Phi'^{(1)}(z) \text{ for } x_2 > 0, \tag{13}$$

$$\bar{\Phi}'^{(1)}(z) = \left(\bar{\mathbf{N}}^{(1)}\right)^{-1}\mathbf{N}^{(2)}\Phi'^{(2)}(z) \text{ for } x_2 < 0. \tag{14}$$

Further we find the jump of the following vector function:

$$\langle \mathbf{v}'(x_1) \rangle = \mathbf{v}'^{(1)}(x_1 + i0) - \mathbf{v}'^{(1)}(x_1 - i0), \tag{15}$$

when passing through the interface. Finding from the formula (9):

$$\mathbf{v}'^{(k)}(x_1 \pm i0) = \mathbf{M}^{(k)}\Phi'^{(k)}(x_1 \pm i0) + \bar{\mathbf{M}}^{(k)}\bar{\Phi}'^{(k)}(x_1 \mp i0)$$

and substituting in (15), one gets:

$$\langle \mathbf{v}'(x_1) \rangle = \mathbf{M}^{(1)}\Phi'^{(1)}(x_1 + i0) + \bar{\mathbf{M}}^{(1)}\bar{\Phi}'^{(1)}(x_1 - i0) -$$

$$- \mathbf{M}^{(2)}\Phi'^{(2)}(x_1 - i0) - \bar{\mathbf{M}}^{(2)}\bar{\Phi}'^{(2)}(x_1 + i0).$$

Determining further:

$$\Phi'^{(2)}(x_1 - i0) = \left(\mathbf{N}^{(2)}\right)^{-1}\bar{\mathbf{N}}^{(1)}\bar{\Phi}'^{(1)}(x_1 - i0)$$

from (14) and substituting this expression together with (13), at $x_2 \to +0$, into the latest formula, leads to:

$$\langle \mathbf{v}'(x_1) \rangle = \mathbf{D}\Phi'^{(1)}(x_1 + i0) + \bar{\mathbf{D}}\bar{\Phi}'^{(1)}(x_1 - i0), \tag{16}$$

where: $\mathbf{D} = \mathbf{M}^{(1)} - \bar{\mathbf{M}}^{(2)}\left(\bar{\mathbf{N}}^{(2)}\right)^{-1}\mathbf{N}^{(1)}$.

Introducing a new vector-function:

$$\mathbf{W}(z) = \begin{cases} \mathbf{D}\Phi'^{(1)}(z), & x_2 > 0, \\ -\bar{\mathbf{D}}\bar{\Phi}'^{(1)}(z), & x_2 < 0 \end{cases} \tag{17}$$

the expression (16) can be written as:

$$\langle \mathbf{v}'(x_1) \rangle = \mathbf{W}^+(x_1) - \mathbf{W}^-(x_1). \tag{18}$$

From the relations (10) we have:

$$\mathbf{P}^{(1)}(x_1, 0) =$$
$$\mathbf{N}^{(1)}\Phi'^{(1)}(x_1 + i0) + \bar{\mathbf{N}}^{(1)}\bar{\Phi}'^{(1)}(x_1 - i0). \tag{19}$$

Taking into account that on the base of (17):

$$\Phi'^{(1)}(x_1 + i0) = \mathbf{D}^{-1}\mathbf{W}(x_1 + i0),$$
$$\bar{\Phi}'^{(1)}(x_1 - i0) = -(\bar{\mathbf{D}}^{-1})^{-1}\mathbf{W}(x_1 - i0),$$

and substituting these relations into (19), leads to:

$$\mathbf{P}^{(1)}(x_1, 0) = \mathbf{S}\mathbf{W}^+(x_1) - \bar{\mathbf{S}}\mathbf{W}^-(x_1), \tag{20}$$

where: $\mathbf{S} = \mathbf{N}^{(1)}\mathbf{D}^{-1}$. From the last relations it follows that:

$$\mathbf{S} = \left[\mathbf{M}^{(1)}\left(\mathbf{N}^{(1)}\right)^{-1} - \overline{\mathbf{M}}^{(2)}\left(\overline{\mathbf{N}}^{(2)}\right)^{-1}\right]^{-1}.$$

The representations (18) and (20) can be used for solving of anti-plane problems for bimaterials with cracks at the interface. However, we transform further these representations to the form, which is more convenient for the solution of the formulated problem.

Consider the matrix $\mathbf{L} = [L_1, L_2, L_3]$ and the composition:

$$\mathbf{L}\mathbf{P}^{(1)}(x_1, 0) = \mathbf{L}\mathbf{S}\mathbf{W}^+(x_1) - \mathbf{L}\overline{\mathbf{S}}\mathbf{W}^-(x_1). \tag{21}$$

Denoting $\mathbf{Y} = [Y_1, Y_2, Y_3] = \mathbf{L}\mathbf{S}$, we introduce the function:

$$F(z) = \mathbf{Y}\mathbf{W}(z). \tag{22}$$

Let's assume that $\mathbf{L}\overline{\mathbf{S}} = -\gamma\mathbf{L}\mathbf{S}$ and transpose last equation for convenience. It gives:

$$(\gamma\mathbf{S}^T + \overline{\mathbf{S}}^T)\mathbf{L}^T = 0. \tag{23}$$

This is an eigenvalue problem for finding an eigenvalue γ and an eigenvector $\mathbf{L}^T$. The eigenvalues are the roots of the equation:

$$\det(\gamma\mathbf{S}^T + \overline{\mathbf{S}}^T) = 0, \tag{24}$$

which we denote as $\gamma_1, \gamma_2, \gamma_3$. Eigenvectors $\mathbf{L}_j^T = \left[L_{j1}, L_{j2}, L_{j3}\right]^T$ $(j = 1,2,3)$, which correspond to the eigenvalues γ_j are found from the system (23).

Denoting:

$$\mathbf{Y}_j = \mathbf{L}_j\mathbf{S}, \tag{25}$$

we obtain from (21):

$$\mathbf{L}_j\mathbf{P}^{(1)}(x_1, 0) = \mathbf{Y}_j\mathbf{W}^+(x_1) + \gamma_j\mathbf{Y}_j\mathbf{W}^-(x_1),$$

or, taking into account (22), one gets:

$$\mathbf{L}_j\mathbf{P}^{(1)}(x_1, 0) = F_j^+(x_1) + \gamma_j F_j^-(x_1), \tag{26}$$

where:

$$F_j(z) = \mathbf{Y}_j\mathbf{W}(z). \tag{27}$$

Because $\mathbf{F}^+(x_1) = \mathbf{F}^-(x_1) = \mathbf{F}(x_1)$ for $x_1 \notin (c, b)$, we obtain from (26) the following condition at infinity:

$$F_j(z)\big|_{z\to\infty} = \frac{1}{1+\gamma_j}\left(L_{j1}\sigma_{32}^\infty + L_{j2}E_1^\infty + L_{j3}H_1^\infty\right). \tag{28}$$

It should be noted that for the considered class of piezoelectric/piezomagnetic materials the matrix $\mathbf{S}$ has the following structure:

$$\mathbf{S} = \begin{pmatrix} i\,s_{11} & s_{12} & s_{13} \\ s_{21} & i\,s_{22} & i\,s_{23} \\ s_{31} & i\,s_{32} & i\,s_{33} \end{pmatrix}, \tag{29}$$

where all s_{kl} $(k, l = 1,2,3)$ are real. In this case the eigenvalues of the system (23) are:

$$\gamma_1 = 1, \gamma_2 = \frac{\delta+1}{\delta-1}, \gamma_3 = \frac{\delta-1}{\delta+1}, \tag{30}$$

where $t_1 = s_{21}s_{32}s_{13} + s_{12}s_{23}s_{31} - s_{31}s_{22}s_{13} - s_{12}s_{21}s_{33}$, $t_2 = s_{11}s_{22}s_{33} - s_{23}s_{32}s_{11}$, $\delta = \sqrt{t_2/t_1}$.

The eigenvectors, corresponding to these eigenvalues are found from the system (23) and can be presented in the form:

$$\mathbf{L}_1 = [0, 1, \omega_{13}], \mathbf{L}_2 = [1, i\omega_{22}, i\omega_{23}],$$

$$\mathbf{L}_3 = [1, i\omega_{32}, i\omega_{33}], \tag{31}$$

where: $\omega_{13} = -\frac{s_{21}}{s_{31}}$, $\omega_{22} = \frac{\omega}{D_0}(s_{12}s_{23} - s_{13}s_{32})$, $\omega_{23} = \frac{\omega}{D_0}(s_{22}s_{13} - s_{23}s_{12})$, $\omega_{32} = -\omega_{22}$, $\omega_{33} = -\omega_{23}, \omega = \frac{\gamma_2+1}{\gamma_2-1}$, $D_0 = s_{22}s_{33} - s_{23}s_{32}$.

Taking into account the presentation (31) the relation (26) for $j = 1,2$ can be written in the form:

$$E_1^{(1)}(x_1, 0) + \omega_{13}H_1^{(1)}(x_1, 0) = F_1^+(x_1) + F_1^-(x_1), \tag{32}$$

$$\sigma_{32}^{(1)}(x_1, 0) + i\omega_{22}E_1^{(1)}(x_1, 0) + i\omega_{23}H_1^{(1)}(x_1, 0) =$$
$$= F_2^+(x_1) + \gamma_2 F_2^-(x_1). \tag{33}$$

From the equations (6), (18) and (27) one gets:

$$Y_{j1}\langle u_3'(x_1, 0)\rangle + Y_{j2}\langle D_2(x_1, 0)\rangle + Y_{j3}\langle B_2(x_1, 0)\rangle =$$
$$= F_j^+(x_1) - F_j^-(x_1). \tag{34}$$

It follows from analysis of (29) and (31) that for the considered class of materials $Y_{11} = 0$, Y_{jk} are real and Y_{1k}, Y_{j1} are pure imaginary. Therefore, introducing the following designations $\eta_{1k} = -iY_{1k}, \eta_{j1} = -iY_{j1}, \eta_{jk} = Y_{jk}$ $(j, k = 2,3)$ the Eq. (34) for $j = 1,2$ can be written in the form:

$$i\eta_{12}\langle D_2(x_1, 0)\rangle + i\eta_{13}\langle B_2(x_1, 0)\rangle = F_1^+(x_1) - F_1^-(x_1), \tag{35}$$

$$i\eta_{21}\langle u_3'(x_1, 0)\rangle + \eta_{22}\langle D_2(x_1, 0)\rangle + \eta_{23}\langle B_2(x_1, 0)\rangle =$$
$$= F_2^+(x_1) - F_2^-(x_1). \tag{36}$$

It's important that all ω_{ij} and η_{ij} in Eqs. (32), (33) and (35), (36) are real.

4. FORMULATION AND SOLUTION OF THE PROBLEMS OF LINER RELATIONSHIP

Satisfying the conditions (14) with use of (33), one gets:

$$F_2^+(x_1) + \gamma_2 F_2^-(x_1) = 0 \text{ for } c < x_1 < a. \tag{37}$$

Satisfying further the conditions (15) by using (33) and (36), we obtain:

$$\text{Re}[F_2^+(x_1) + \gamma_2 F_2^-(x_1)] = 0,$$

$$\text{Re}[F_2^+(x_1) - F_2^-(x_1)] = 0 \text{ for } a < x_1 < b.$$

The last equation can be written in the form:

$$\text{Re}F_2^\pm(x_1) = 0 \quad \text{for } a < x_1 < b. \tag{38}$$

The equations (37), (38) form the combined Dirichlet-Riemann boundary value problem. To solve this problem we introduce the following substitution:

$$F_2(z) = i\Phi_2(z) \tag{39}$$

and Eqs. (37), (38) attain the form:

$$\Phi_2^+(x_1) + \gamma_2\Phi_2^-(x_1) = 0, c < x_1 < a,$$

$$\text{Im}\Phi_2^+(x_1) = 0, a < x_1 < b. \tag{40}$$

On the base of (28) and (39) the conditions at infinity can be presented in the form:

$$\Phi_2(z)|_{z\to\infty} = \tilde{E}_2 + \tilde{H}_2 - i\tilde{\sigma}_{32}^{(1)}, \tag{41}$$

where $\tilde{E}_2 = \frac{\omega_{22}}{1+\gamma_2}E_1^\infty$, $\tilde{H}_2 = \frac{\omega_{23}}{1+\gamma_2}H_1^\infty$, $\tilde{\sigma}_{32}^{(2)} = \frac{\sigma_{32}^\infty}{1+\gamma_2}$.

Considering the results of Nahmein and Nuller (1986) and Kozinov et al., (2013) the solution of the problem (40) under the conditions at infinity (41) has the following form:

$$\Phi_2(z) = P(z)X_1(z) + Q(z)X_2(z), \tag{42}$$

where: $P(z) = C_1 z + C_2$, $Q(z) = D_1 z + D_2$, $l = b - c$,

$$X_1(z) = \frac{ie^{i\chi(z)}}{\sqrt{(z-c)(z-b)}}, X_2(z) = \frac{e^{i\chi(z)}}{\sqrt{(z-c)(z-a)}},$$

$$\chi(z) = 2\varepsilon_2\ln\frac{\sqrt{(b-a)(z-c)}}{\sqrt{l(z-a)}+\sqrt{(a-c)(z-b)}}, \varepsilon_2 = \frac{1}{2\pi}\ln\gamma_2,$$

$$C_1 = -\tilde{\sigma}_{32}\cos\beta - (\tilde{E}_2 + \tilde{H}_2)\sin\beta, C_2 = -\frac{c+b}{2}C_1 - \beta_1 D_1,$$

$$D_1 = (\tilde{E}_2 + \tilde{H}_2)\cos\beta - \tilde{\sigma}_{32}\sin\beta, D_2 = \beta_1 C_1 - \frac{c+a}{2}D_1.$$

In the above relations:

$$\beta = \varepsilon_2\ln\frac{1-\sqrt{1-\lambda}}{1+\sqrt{1-\lambda}}, \beta_1 = \varepsilon_2\sqrt{(a-c)(b-c)}, \lambda = (b-a)/l.$$

Using presentation (33) one can write:

$$\sigma_{32}^{(1)}(x_1, 0) + i\omega_{22}E_1^{(1)}(x_1, 0) + i\omega_{23}H_1^{(1)}(x_1, 0) =$$
$$= i[\Phi_2^+(x_1) + \gamma_2\Phi_2^-(x_1)]. \tag{43}$$

The stress $\sigma_{32}^{(1)}(x_1, 0)$ can be found from (43), however only the combination of $E_1^{(1)}(x_1, 0)$ and $H_1^{(1)}(x_1, 0)$ can be obtained as imaginary part of this expression. To find the mentioned values separately consider the expressions (32) and (35).

Satisfying with use of (32) to second and third boundary conditions of (4) one arrives at the following equation:

$$F_1^+(x_1) + F_1^-(x_1) = 0 \text{ for } c < x_1 < a. \tag{44}$$

Due to second and third boundary conditions of (5) the function $F_1(z)$ is analytic in the whole plane except the segment $[c, a]$. Taking this fact into account, the solution of Eq. (44) can be presented in the form Muskhelishvili (1977):

$$F_1(z) = \frac{c_0 + c_1 z}{\sqrt{(z-c)(z-a)}},$$

where c_0 and c_1 are arbitrary constants. Determining these constants from the condition at infinity $F_1(z)|_{z\to\infty} = 0.5(E_1^\infty + \omega_{13}H_1^\infty)$, which follows from (32), and from the requirement of single valuedness of displacements, one gets:

$$F_1(z) = (E_1^\infty + \omega_{13}H_1^\infty)\frac{z-(a+c)/2}{2\sqrt{(z-c)(z-a)}}. \tag{45}$$

Using the solutions (42), (45) and the presentations (35), (36), we get the following system for u_3, D_2, B_2 determination at $x_1 \in (c, a)$:

$$i\eta_{21}\langle u'_3(x_1, 0)\rangle + \eta_{22}\langle D_2(x_1, 0)\rangle + \eta_{23}\langle B_2(x_1, 0)\rangle =$$
$$= i\sqrt{\alpha}\left[\frac{P(x_1)}{\sqrt{b-x_1}} - i\frac{Q(x_1)}{\sqrt{a-x_1}}\right]\frac{\exp[i\chi^*(x_1)]}{\sqrt{x_1-c}}, \tag{46}$$

$$i\eta_{12}\langle D_2(x_1, 0)\rangle + i\eta_{13}\langle B_2(x_1, 0)\rangle =$$

$$= (E_1^\infty + m_{13}H_1^\infty) \cdot \frac{x_1-(a+c)/2}{\sqrt{(x_1-c)(x_1-a)}}, \tag{47}$$

where: $\alpha = \frac{(1+\gamma_2)^2}{4\gamma_2}$,

$$\chi^*(x_1) = 2\varepsilon_2\ln\left[\frac{\sqrt{(b-a)(x_1-c)}}{\sqrt{(b-c)(a-x_1)}+\sqrt{(a-c)(b-x_1)}}\right].$$

From Eq. (46) one gets the following expression for the displacement jump at the segment (c, a):

$$\langle u'_3(x_1, 0)\rangle = \frac{2\sqrt{\alpha}}{\eta_{21}\sqrt{x_1-c}}\left(\frac{P(x_1)\cos\chi^*(x_1)}{\sqrt{b-x_1}} + \frac{Q(x_1)\sin\chi^*(x_1)}{\sqrt{a-x_1}}\right)$$

Integrating this equation, one arrives at:

$$\langle u_3(x_1, 0)\rangle = \int_c^{x_1}\left[\frac{2\sqrt{\alpha}}{\eta_{21}\sqrt{t-c}}\left(\frac{P(t)\cos\chi^*(t)}{\sqrt{b-t}} + \right.\right.$$
$$\left.\left. +\frac{Q(t)\sin\chi^*(t)}{\sqrt{a-t}}\right)\right]dt, c < x_1 < a. \tag{48}$$

and also the real part of (46) and imaginary part of (47) lead to the following system of equations at the interval $x_1 \in (c, a)$:

$$\eta_{12}\langle D_2(x_1, 0)\rangle + \eta_{13}\langle B_2(x_1, 0)\rangle =$$
$$= -(E_1^\infty + \omega_{13}H_1^\infty) \cdot \frac{x_1-(a+c)/2}{\sqrt{(x_1-c)(a-x_1)}},$$

$$\eta_{22}\langle D_2(x_1, 0)\rangle + \eta_{23}\langle B_2(x_1, 0)\rangle =$$
$$= -\frac{P_2(x_1)}{\sqrt{b-x_1}}\sin\chi^*(x_1) + \frac{Q_2(x_1)}{\sqrt{a-x_1}}\cos\chi^*(x_1). \tag{49}$$

From this system the expressions for $\langle D_2(x_1, 0)\rangle$ and $\langle B_2(x_1, 0)\rangle$ at the interval (c, a) can be easily found.

With use of (42), it follows from (33) for $x_1 > b$:

$$\sigma_{32}^{(1)}(x_1, 0) + i\left(\omega_{22}E_1^{(1)}(x_1, 0) + \omega_{23}H_1^{(1)}(x_1, 0)\right) =$$
$$= i\left[\frac{Q(x_1)}{\sqrt{x_1-a}} + \frac{iP(x_1)}{\sqrt{x_1-b}}\right]\frac{(1+\gamma_2)\exp[i\chi(x_1)]}{\sqrt{x_1-c}}.$$

From this equation the expression for the stress at the crack continuation can be written in the form:

$$\sigma_{32}^{(1)}(x_1, 0) = -(1 + \gamma_2)\left(\frac{Q(x_1)}{\sqrt{x_1-a}} \cdot \frac{\sin[\chi(x_1)]}{\sqrt{x_1-c}} + \right.$$
$$\left. +\frac{P(x_1)}{\sqrt{x_1-b}} \cdot \frac{\cos\chi(x_1)}{\sqrt{x_1-c}}\right), x_1 > b. \tag{50}$$

For electrical and magnetic fields at the crack continuation $x_1 > b$ one arrives at the following system:

$$E_1^{(1)}(x_1, 0) + \omega_{13}H_1^{(1)}(x_1, 0) =$$
$$= (E_1^\infty + m_{13}H_1^\infty)\frac{x_1-(a+c)/2}{\sqrt{(x_1-c)(x_1-a)}}, \tag{51}$$

$$\omega_{22}E_1^{(1)}(x_1, 0) + \omega_{23}H_1^{(1)}(x_1, 0) =$$
$$= \frac{(1+\gamma_2)}{\sqrt{x_1-c}} \cdot \left(\frac{Q(x_1)}{\sqrt{x_1-a}}\cos[\chi(x_1)] - \frac{P(x_1)}{\sqrt{x_1-b}}\sin[\chi(x_1)]\right). \tag{52}$$

From the last system the expressions for $E_1^{(1)}(x_1, 0)$ and $H_1^{(1)}(x_1, 0)$ at $x_1 > b$ can be easily found.

Consider now the interval (a, b). Taking into account that at this interval (Herrmann and Loboda, 2003):

$$X_1^\pm(x_1) = \frac{\pm e^{\pm\chi_0(x_1)}}{\sqrt{(x_1-c)(b-x_1)}}, \quad X_2^\pm(x_1) = \frac{e^{\pm\chi_0(x_1)}}{\sqrt{(x_1-c)(x_1-a)}},$$

where: $\chi_0(x_1) = 2\varepsilon_2 \tan^{-1}\sqrt{\frac{(a-c)(b-x_1)}{(b-c)(x_1-a)}}$ and using (42), one can write

$$\Phi_2^\pm(x_1) = \pm\frac{e^{\pm\chi_0(x_1)}P(x_1)}{\sqrt{(x_1-c)(b-x_1)}} + \frac{e^{\pm\chi_0(x_1)}Q(x_1)}{\sqrt{(x_1-c)(x_1-a)}}. \tag{53}$$

Substituting (53) into (36), (39) and taking into account that $\langle D_2(x_1,0)\rangle = 0$, $\langle B_1(x_1,0)\rangle = 0$ at (a,b) we obtain the following expression for the displacement jump:

$$\langle u'_3(x_1,0)\rangle = \frac{2}{\eta_{21}\sqrt{x_1-c}}\left(\frac{P(x_1)}{\sqrt{b-x_1}}\cosh\chi_0(x_1) + \right.$$

$$\left. + \frac{Q(x_1)}{\sqrt{x_1-a}}\sinh\chi_0(x_1)\right), a < x_1 < b.$$

Integrating this equation, one arrives at:

$$\langle u_3(x_1,0)\rangle = \int_b^{x_1}\left[\frac{2}{\eta_{21}\sqrt{t-c}}\left(\frac{P(t)}{\sqrt{b-t}}\cosh\chi_0(t) + \right.\right.$$

$$\left.\left. + \frac{Q(t)}{\sqrt{t-a}}\sinh\chi_0(t)\right)\right]dt, a < x_1 < b. \tag{54}$$

The formulas (32), (33) give for $a < x_1 < b$ the equation (51) and the following expression:

$$\omega_{22}E_1^{(1)}(x_1,0) + \omega_{23}H_1^{(1)}(x_1,0) =$$

$$= \frac{P(x_1)}{\sqrt{(x_1-c)(b-x_1)}}\left(e^{\chi_0(x_1)} - \gamma_2 e^{-\chi_0(x_1)}\right) +$$

$$+ \frac{Q(x_1)}{\sqrt{(x_1-c)(x_1-a)}}\left(e^{\chi_0(x_1)} + \gamma_2 e^{-\chi_0(x_1)}\right). \tag{55}$$

From the system (51), (55) the expressions for $E_1^{(1)}(x_1,0)$ and $H_1^{(1)}(x_1,0)$ at $a < x_1 < b$ can be easily found.

5. STRESS, ELECTRIC AND MAGNETIC INTENSITY FACTORS

Analysis of the formulas (47)-(49) and (52), (53) shows that the stress $\sigma_{32}^{(1)}(x_1,0)$ is singular for $x_1 \to b + 0$, $E_1^{(1)}(x_1,0)$, $H_1^{(1)}(x_1,0)$ are singular for $x_1 \to a + 0$ and $x_1 \to b - 0$, and also $\langle D_2(x_1,0)\rangle$, $\langle B_2(x_1,0)\rangle$ are singular for $x_1 \to a - 0$. In all mentioned cases, a square root singularity takes place. Therefore, introducing the following stress and electrical intensity factors (IFs):

$$K_3 = \lim_{x_1\to b+0}\sqrt{2\pi(x_1-b)}\sigma_{32}(x_1,0),$$

$$K_E^a = \lim_{x_1\to a+0}\sqrt{2\pi(x_1-a)}E_1^{(1)}(x_1,0),$$

$$K_H^a = \lim_{x_1\to a+0}\sqrt{2\pi(x_1-a)}H_1^{(1)}(x_1,0),$$

$$K_E^b = \lim_{x_1\to b-0}\sqrt{2\pi(b-x_1)}E_1^{(1)}(x_1,0),$$

$$K_H^b = \lim_{x_1\to b-0}\sqrt{2\pi(b-x_1)}H_1^{(1)}(x_1,0),$$

$$K_D^a = \lim_{x_1\to a-0}\sqrt{2\pi(a-x_1)}\langle D_2(x_1,0)\rangle,$$

$$K_B^a = \lim_{x_1\to a-0}\sqrt{2\pi(a-x_1)}\langle B_2(x_1,0)\rangle$$

and using formulas (50), (51), (55) and (48), (49), one obtains:

$$K_3 = -\frac{(1+\gamma_2)\sqrt{2\pi}}{\sqrt{b-c}}P(b),$$

$$K_E^a + \omega_{13}K_H^a = \sqrt{\frac{\pi(a-c)}{2}}(E_1^\infty + \omega_{13}H_1^\infty),$$

$$\omega_{22}K_E^a + \omega_{23}K_H^a = \sqrt{\frac{2\pi}{a-c}}(1+\gamma_2)Q(a), \tag{56}$$

$$K_E^b + \omega_{13}K_H^b = 0,$$

$$\omega_{22}K_E^b + \omega_{23}K_H^b = \sqrt{\frac{2\pi}{b-c}}(1-\gamma_2)P(b), \tag{57}$$

$$\eta_{12}K_D^a + \eta_{13}K_B^a = -(E_1^\infty + \omega_{13}H_1^\infty)\sqrt{\pi(a-c)/2},$$

$$\eta_{22}K_D^a + \eta_{23}K_B^a = \sqrt{2\pi}Q(a). \tag{58}$$

Substituting the expressions for $P(b)$ from (42), we obtain the following formula:

$$K_3 = \sqrt{\frac{\pi l}{2}}\{-\sigma_{32}^\infty\cos\beta - (\omega_{22}E_1^\infty + \omega_{23}H_1^\infty)\sin\beta -$$

$$-2\varepsilon_2\sqrt{1-\lambda}[-\sigma_{32}^\infty\sin\beta + (\omega_{22}E_1^\infty + \omega_{23}H_1^\infty)\cos\beta]\}. \tag{59}$$

The intensity factors K_E^a and K_H^a, K_E^b and K_H^b, K_D^a and K_B^a can be found from the systems (56), (57), (58), respectively.

At the left crack tip c, an oscillating singularity takes place. Such singularity for a conductive interface crack in an anti-plane case of a piezoelectric material has been already analyzed in papers by Wang et al., (2003) and Wang and Zhong (2002). For this reason, we do not pay special attention to this singularity here. At the right crack tip, the same oscillating singularity will take place only if $a = b$, i.e. if the permeable part of the crack is absent. In a more general case, which is studied in this paper, i.e. for zone $[a,b]$ having nonzero length, the previously mentioned oscillating singularity at the point $a = b$ transforms into two square root singularities at two different points a and b with intensity factors defining by Eqs. (56)-(59). Similar situation has been studied for an antiplane case of a piezoelectric material by Lapusta et al., (2017) and also it is similar to the case of a frictionless contact zone at the interface crack tip for a plane problem (Comninou, 1977).

6. NUMERICAL REALIZATION

For the numerical analysis the materials with the following characteristics (Sih and Song, 2003) were chosen:

$$c_{44}^{(1)} = 43.7\cdot 10^9[Pa], e_{15}^{(1)} = 17[C/m^2],$$

$$\alpha_{11}^{(1)} = 15.1\cdot 10^{-9}\left[\frac{C}{V\cdot m}\right], \quad d_{11}^{(1)} = 0, \; h_{15}^{(1)} = 165\left[\frac{N}{a\cdot m}\right],$$

$$\gamma_{11}^{(1)} = 180.5\cdot 10^{-6}\left[\frac{N\cdot s^2}{c^2}\right], \; c_{44}^{(2)} = 42.47\cdot 10^9[Pa],$$

$$e_{15}^{(2)} = -0.48[C/m^2], \quad \alpha_{11}^{(2)} = 0.0757\cdot 10^{-9}\left[\frac{C}{V\cdot m}\right],$$

$$d_{11}^{(2)} = 0, h_{15}^{(2)} = 385\left[\frac{N}{a\cdot m}\right], \gamma_{11}^{(2)} = 414.5\cdot 10^{-6}\left[\frac{N\cdot s^2}{c^2}\right]$$

and $c = -0.01m$, $b = 0.01\ m$, $\lambda = 0{,}1$.
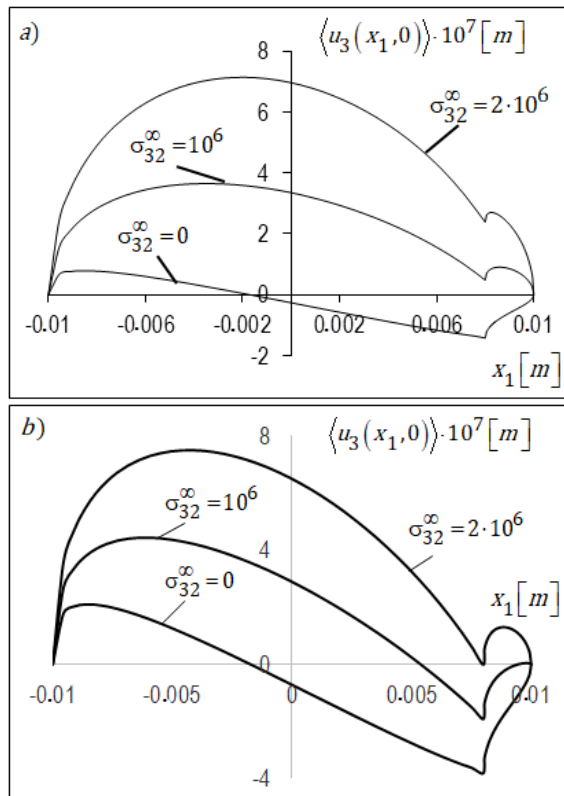

Fig. 2. The displacement jump at the segment $[c, b]$
for $E_1^\infty = 9 \cdot 10^3 [V/m]$, $H_1^\infty = 0$ (a)
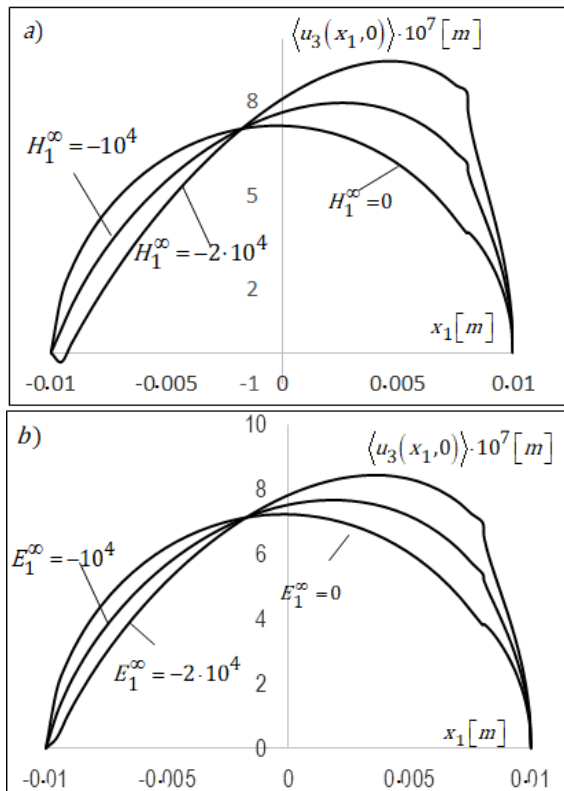and $E_1^\infty = 0$, $H_1^\infty = 1.7 \cdot 10^4 [A/m]$ (b)

Fig. 3. The displacement jump at the segment $[c, b]$ for different
vaues of $H_1^\infty [A/m]$ (a) and $E_1^\infty [V/m]$(b)

The crack sliding for $E_1^\infty = 9 \cdot 10^3 [V/m]$, $H_1^\infty = 0$ and $E_1^\infty = 0$, $H_1^\infty = 1.7 \cdot 10^4 [A/m]$ and different values of $\sigma_{32}^\infty [Pa]$ are presented in Figures 2a and 2b, respectively. It can be seen from these Figures that even for zero mechanical loading σ_{32}^∞ the crack faces slide with respect to each other due to non-zero electric (Fig. 2a) or magnetic (Fig. 2b) fields.

The crack sliding for $\sigma_{32}^\infty = 2 \cdot 10^6 [Pa]$ and different values of $H_1^\infty [A/m]$ and $E_1^\infty [V/m]$ are presented in Figs. 3a and 3b, respectively.

It should be mention that the oscillating singularity takes place at the left crack tip. However for the presented model of the crack sliding the oscillating singularity is physically admissible because the faces can slide relative to each other in any direction. One of the appearances the negative crack faces jump (analogy of the oscillating singularity) can be seen for the lower lines at the left crack tip in Fig. 3a.
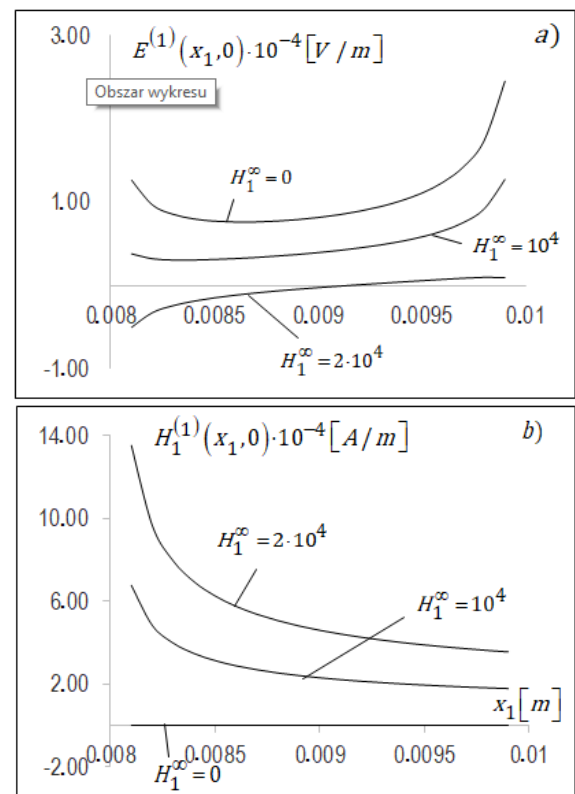

Fig. 4. The variation of the electric $E_1^{(1)}(x_1, 0)$ (a) and magnetic
$H_1^{(1)}(x_1, 0)$ (b) fields along the electro-magnetically permeable
crack region (a, b)

The variation of the electric $E_1^{(1)}(x_1, 0)$ and magnetic $H_1^{(1)}(x_1, 0)$ fields along the electro-magnetically permeable crack region (a, b) are shown in Figs. 4a and 4b, respectively, for $\lambda = 0.1$, $\sigma_{32}^\infty = 10^6 [Pa]$, $E_1^\infty = 0$ and different values of $H_1^\infty [A/m]$. It is seen from these figures that $E_1^{(1)}(x_1, 0)$ and $H_1^{(1)}(x_1, 0)$ is almost equal to 0 for $E_1^\infty = 0$ and $H_1^\infty = 0$, but they become rather large for a nonzero external magnetic field. Besides, $E_1^{(1)}(x_1, 0)$ and $H_1^{(1)}(x_1, 0)$ are singular at both ends of the segment $[a, b]$.

Consider further the behavior of mechanic, electric and magnetic values at the crack continuation. Fig. 5 show the stress $\sigma_{32}^{(1)}(x_1, 0)$ variations in this zone for $E_1^\infty = 9 \cdot 10^3 [V/m]$,

$H_1^\infty = 0$ (a) and $E_1^\infty = 0$, $H_1^\infty = 1.7 \cdot 10^4 [A/m]$ (b) and different values of $\sigma_{32}^\infty [Pa]$.
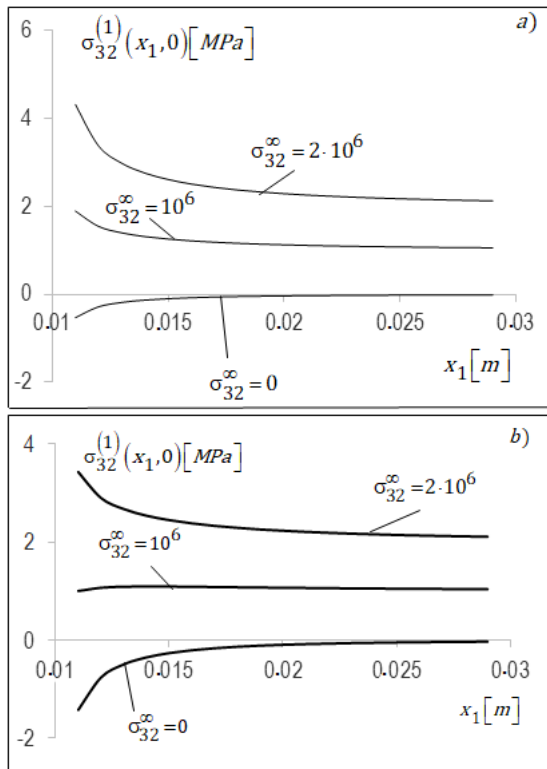

Fig. 5. The stress $\sigma_{32}^{(1)}(x_1, 0)$ variations on (a, b)
for $E_1^\infty = 9 \cdot 10^3 [V/m]$, $H_1^\infty = 0$ (a) and $E_1^\infty = 0$,
$H_1^\infty = 1.7 \cdot 10^4 [A/m]$ (b) and different values of σ_{32}^∞
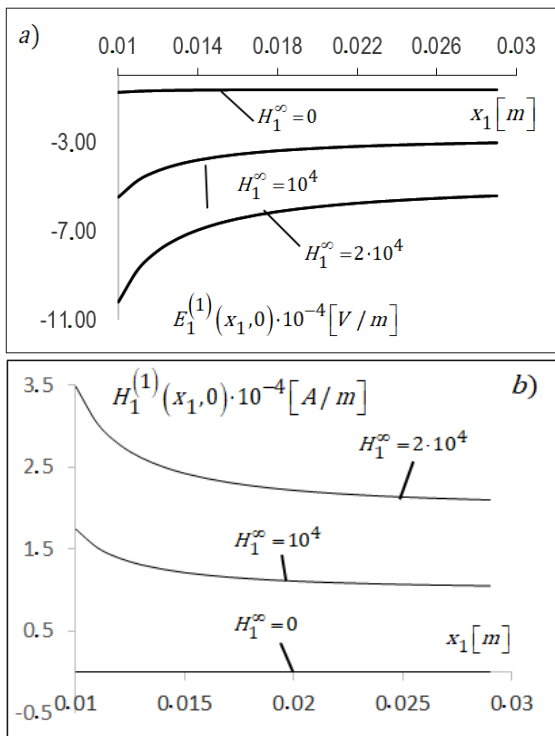

Fig. 6. The variation of the electric $E_1^{(1)}(x_1, 0)$ (a) and magnetic
$H_1^{(1)}(x_1, 0)$ (b) fields along the crack continuation $b > 0$
for $\lambda = 0.1$, $\sigma_{32}^\infty = 10^6 [Pa]$, $E_1^\infty = 0$ and different values
of H_1^∞

The variation of the electric $E_1^{(1)}(x_1, 0)$ and magnetic $H_1^{(1)}(x_1, 0)$ fields along the crack continuation $b > 0$ are shown in Figs. 6a and 6b, respectively, for $\lambda = 0.1$, $\sigma_{32}^\infty = 10^6 [Pa]$, $E_1^\infty = 0$ and different values of $H_1^\infty [A/m]$. It is seen from these figures that $H_1^{(1)}(x_1, 0)$ is almost equal to 0 for $E_1^\infty = 0$ and $H_1^\infty = 0$, but $E_1^{(1)}(x_1, 0)$ decreases on modulus while $H_1^{(1)}(x_1, 0)$ increases with growing of H_1^∞.

Variations of the normalized stress intensity factor (SIF) K_3 is shown in Tables 1 for $\sigma_{32}^\infty = 10^6 [Pa]$, $E_1^\infty = 0$ and different values of λ and H_1^∞. It can be seen that for each λ the decreasing of magnetic field H_1^∞ (growing it on modules) leads to decreasing of the SIF K_3 and even to turning it into zero for $\lambda = 0.1$ and $H_1^\infty = -18742 [A/m]$. It means that electric and magnetic fields can be used for governing of the SIF and decreasing the probability of fracture.

Tab. 1. Variations of the normalized stress intensity factor (SIF) K_3

λ H^∞	0.1	0.2	0.3
0	177676.	181031.	181731.
-5000	130277.	150716.	160997.
-10000	82877.8	120401.	140263.
-15000	35478.5	90086.	119529.
-18742.6	0.0	67394.7	104009.

To control the obtained analytical solution the numerical experiment has been performed. The finite sized body composed of two piezoelectric parallelepipeds $-30mm \leq x_1 \leq 30mm$, $0 \leq x_2 \leq 20mm$, $0 \leq x_3 \leq 180mm$ and $-30mm \leq x_1 \leq 30mm$, $-20mm \leq x_2 \leq 0$, $0 \leq x_3 \leq 180mm$ with the same piezoelectric material parameters as above is considered. A crack in the region $-10mm \leq x_1 \leq 10mm$, $x_2 = 0$, $0 \leq x_3 \leq 180mm$ is situated. It is assumed that for $-10mm \leq x_1 \leq 5mm$ the faces of the crack are conductive while in the remaining part they are permeable. The lower boundary $x_2 = -20mm$ was fixed while to the upper one $x_2 = 20mm$ the uniformly distributed shear stress $\sigma_{32}^{(1)}(x_1, 20) = 10MPa$ was applied. The finite element ABAQUS code was used for the solution of this problem. The mesh grinding at the crack tips was done. As a result of this solution the maximum value of the crack sliding at the point $x_1 = x_2 = 0$, $x_3 = 90mm$ turned out to be $4.93 \times 10^{-4} mm$. Analytical analysis performing for the same loading, materials, conducting and permeable zone lengths gave the result 4.61×10^{-4} mm for the crack sliding at the same point. Taking into account that we compared the results for finite size domain (with a crack 3 times shorter than the width of the compound) and for infinite domain, the obtained error in 6.51% can be considered as quite satisfactory. Therefore, this numerical test confirms the validity of the analytical approach developed in this paper.

7. CONCLUSIONS

An interface crack $c \leq x_1 \leq b$, $x_2 = 0$ between two semi-infinite piezoelectric/piezomagnetic spaces $x_2 > 0$ and $x_2 < 0$

under out-of-plane mechanical load and in-plane electrical and magnetic fields parallel to the crack faces is considered. The part (c, a) of the crack $(a \leq b)$ faces is assumed to be electrically conductive and having uniform distribution of magnetic potential on it faces. The remaining part of the crack faces is electrically and magnetically permeable. Such situation can occur because of a soft multi-layered electrode exfoliation, made of ferromagnetic material, situated at the interval $[c, a]$, with additional exfoliation of the interval $[a, b]$ of the non-electroded interface. The considered problem involves the mixed electric and magnetic conditions at the crack faces and is much more complicated than the traditional formulation of the interface crack problem for a conductive crack.

The presentations (32), (33) and (35), (36) were formulated for mechanical, electrical, and magnetic factors via a functions which are analytic in the whole plane except the crack region. With these representations the combined Dirichlet-Riemann boundary value problem (37), (38) and Hilbert problem (44) are formulated and solved in the form of relatively simple analytical formulas for any position of the point a. Due to this solution analytical expressions for stress, electric and magnetic fields as well as for the crack faces displacement jump are presented. The singularities of the obtained solution at the points a and b are investigated and the formulas for the corresponding intensity factors are presented. In Figures 2-6 the variations of the mechanic, electric and magnetic quantities along the appropriate parts of the interface are illustrated for certain materials combinations and for certain positions of the point a. The stress intensity factor corresponding to the results of Figs. 2-6 are given in Tab. 1.

The results of analytical and numerical analysis showed that both electric and magnetic fields essentially influence the mechanical, electrical and magnetic fields at the crack tip. It follows from this results that the mentioned fields can be used for decreasing of the stress intensity factor and consequently for the decreasing of failure dangerous of electronic devices working under the action of the mention fields.

REFERENCES

1. **Beom H. G., Atluri S. N.** (2002), Conducting cracks in dissimilar piezoelectric media, *International Journal of Fracture*, 118, 285–301.
2. **Chen H., Wei W., Liu J., Fang D.** (2012), Propagation of a mode-III interfacial crack in a piezoelectric-piezomagnetic bi-material, *Int. J. Solids Struct.*, 49, 2547–2558.
3. **Comninou M.** (1977), The interface crack, *Trans. ASME. Ser. E, J. Applied Mechanics*, 44(4), 631–636.
4. **Fan C., Zhou Y., Wang H., Zhao M.** (2009), Singular behaviors of interfacial cracks in 2D magnetoelectroelastic bimaterials, *Acta Mech. Solida Sinica*, 22, 232-239.
5. **Feng W. J., Ma P., Pan E. N., Liu J. X.** (2011), A magnetically impermeable and electrically permeable interface crack with a contact zone in a magnetoelectroelastic bimaterial under concentrated magnetoelectromechanical loads on the crack faces, *Sci. China Ser. G*, 54, 1666-1679.
6. **Feng W. J., Ma P., Su R. K. L.** (2012), An electrically impermeable and magnetically permeable interface crack with a contact zone in magnetoelectroelastic bimaterials under a thermal flux and magnetoelectromechanical loads, *Int. J. Solids Structures*, 49, 3472-3483.
7. **Feng W. J., Su R. K. L., Liu J. X., Li Y. S.** (2010), Fracture analysis of bounded magnetoelectroelastic layers with interfacial cracks under magnetoelectromechanical loads: plane problem, *J. Intell. Mater. Syst. Struct.*, 21, 581-594.
8. **Govorukha V., Kamlah M., Loboda V., Lapusta Y.** (2016), Interface cracks in piezoelectric materials, *Smart Mater. Struct.*, 25, 023001 (20pp).
9. **Herrmann K. P., Loboda V. V.** (2003), Fracture mechanical assessment of interface cracks with contact zones in piezoelectric bimaterials under thermoelectromechanical loadings, I. Electrically permeable interface cracks, *Int. J. Solids and Structures*, 40, 4191-4217.
10. **Herrmann K. P., Loboda V. V., Khodanen T. V.** (2010), An interface crack with contact zones in a piezoelectric/piezomagnetic bimaterial, *Archive of Applied Mechanics*, 80(6), 651-670.
11. **Hu K., Chen Z.** (2010), An interface crack moving between magnetoelectroelastic and functionally graded elastic layers, *Appl. Math. Modelling*, 38, 910-925.
12. **Kozinov S., Loboda V., Lapusta Y.** (2013), Periodic set of limited electrically permeable interface cracks with contact zones, *Mech. Res. Communic.*, 48, 32-41.
13. **Lapusta Y., Onopriienko O., Loboda V.** (2017), An interface crack with partially electrically conductive crack faces under antiplane mechanical and in-plane electric loadings, *Mech. Res. Commun.*, 81, 38–43.
14. **Li R., Kardomateas G. A.** (2006), The mode III interface crack in piezo-electro-magneto-elastic dissimilar bimaterials, *J. Appl. Mech.*, 73, 220–227.
15. **Li Y. D., Lee K. Y.** (2010), Effects of magneto-electric loadings and piezomagnetic/piezoelectric stiffening on multiferroic interface fracture, *Eng. Fract. Mech.*, 77, 856-866.
16. **Loboda V., Sheveleva A., Lapusta Y.** (2014), An electrically conducting interface crack with a contact zone in a piezoelectric bimaterial, *Int. J. Solids Struct.*, 51, 63–73.
17. **Ma P., Feng W. J., Su R. K. L.** (2012), An electrically impermeable and magnetically permeable interface crack with a contact zone in a magnetoelectroelastic bimaterial under uniform magnetoelectromechanical loads, *Eur. J. Mech. A/Solids*, 32, 41-51.
18. **Ma P., Feng W. J., Su R. K. L.** (2013), Pre-fracture zone model on electrically impermeable and magnetically permeable interface crack between two dissimilar magnetoelectroelastic materials, *Eng. Fract. Mech.*, 102, 310-323.
19. **Ma P., Feng W., Su R. K. L.** (2011), Fracture assessment of an interface crack between two dissimilar magnetoelectroelastic materials under heat flow and magnetoelectromechanical loadings, *Acta Mech. Solida Sinica*, 24, 429-438.
20. **Muskhelishvili N. I.** (1977), *Some Basic Problems of Mathematical Theory of Elasticity*, Noordhoff International Publishing, Leyden.
21. **Nahmein E. L., Nuller B. M.** (1986), Contact of an elastic half plane and a particularly unbonded stamp [in russian], *Prikladnaja matematica i mechanika*, 50, 663–673.
22. **Parton V. Z., Kudryavtsev B. A.** (1988), *Electromagnetoelasticity*, Gordon and Breach Science Publishers, New York.
23. **Ru C. Q.** (2000), Electrode-ceramic interfacial cracks in piezoelectric multilayer materials, *ASME J. Appl. Mech.*, 67, 255–261.
24. **Shi P. P., Sun S., Li X.** (2013), The cyclically symmetric cracks on the arc-shaped interface between a functionally graded magneto-electro-elastic layer and an orthotropic elastic substrate under static anti-plane shear load, *Eng. Fract. Mech.*, 105, 238-249.
25. **Sih G. C., Song Z. F.** (2003), Magnetic and electric poling effects associated with crack growth in $BaTiO_3$–$CoFe_2O_4$ composite, *Theoretical and Applied Fracture Mechanics*, 39, 209–227.
26. **Su R. K. L., Feng W. J.** (2008), Fracture behavior of a bonded magneto-electro-elastic rectangular plate with an interface crack, *Arch. Appl. Mech.*, 78, 343–362.
27. **Sulym H. T., Piskozub L. G., Piskozub Y. Z., Pasternak Ya. M**. (2015a), Antiplane deformation of a bimaterial containing an interfacial crack with the account of friction. I. Single loading, *Acta Mechanica et Automatica*, 9(2), 115-121.
28. **Sulym H. T., Piskozub L. G., Piskozub Y. Z., Pasternak Ya. M.** (2015b), Antiplane deformation of a bimaterial containing an interfacial crack with the account of friction. 2. Repeating and cyclic loading, *Acta Mechanica et Automatica*, 9(3), 178-184.

29. **Wan Y, Yue Y, Zhong Z.** (2012a), Multilayered piezomagnetic/ piezoelectric composite with periodic interface cracks under magnetic or electric field, *Eng. Fract. Mech.*, 84, 132–145.

30. **Wan Y., Yue Y., Zhong Z.** (2012b), A mode III crack crossing the magnetoelectroelastic bimaterial interface under concentrated magnetoelectromechanical loads, *Int. J. Solids Structures*, 49, 3008-3021.

31. **Wang B. L., Mai Y. W.** (2006), Closed-form solution for an antiplane interface crack between two dissimilar magnetoelectroelastic layers, *J. Appl. Mech.*, 73, 281–290.

32. **Wang B. L., Mai Y. W.** (2008), An exact analysis for mode III cracks between two dissimilar magneto-electro-elastic layers*, Mech. Compos. Mater.*, 44, 533–548.

33. **Wang X., Zhong Z.** (2002), A conducting arc crack between a circular piezoelectric inclusion and an unbounded matrix, *Int. J. Solids Struct.*, 39, 5895–5911.

34. **Wang X., Zhong Z., Wu F. L.** (2003), A moving conducting crack at the interface of two dissimilar piezoelectric materials, *Int. J. Solids Struct.*, 40, 2381–2399.

35. **Yue Y., Wan Y.** (2014), Multilayered piezomagnetic/piezoelectric composite with periodic interfacial Yoffe-type cracks under magnetic or electric field, *Acta Mech.*, 225, 2133-2150.

36. **Zhou Z. G., Chen Y., Wang B.** (2007), The behavior of two parallel interface cracks in magneto-electro-elastic materials under an anti-plane shear stress loading, *Compos. Struct.*, 77, 97–103.

37. **Zhou Z. G., Wang B., Sun Y. G.** (2004), Two collinear interface cracks in magneto-electro-elastic composites, *Int. J. Eng. Science*, 42, 1155–1167.

38. **Zhou Z. G., Wang J. Z., Wu L. Z.** (2009), The behavior of two parallel non-symmetric interface cracks in a magneto-electro-elastic material strip under an anti-plane shear stress loading, *Int. J. Appl. Electromagn. Mech.*, 29, 163–184.

39. **Zhou Z. G., Zhang P. W., Wu L. Z.** (2007), Solutions to a limited-permeable crack or two limited-permeable collinear cracks in piezoelectric/piezomagnetic materials, *Arch. Appl. Mech.*, 77, 861–882.